Title	**Retrieval of the aerosol Inherent Optical Properties: The new WOPAER processing chain**
Version	0.1
Author(s) and affiliation(s)	O. Aznay, F. Zagolski and R. Santer ADRINORD
Distribution	Public report

Executive summary

The AERONET network provides in different stations of the 2Seas region routine measurements. WOPAER is a processing chain which analyzes them to provide the elementary optical properties of the aerosols. An update version of WOPAER was developed and used to analyze the optical properties of our coastal aerosols.

Acronyms

AERONET	AErosol RObotic NETwork
ALM	Almucantar
AOT	Aerosol Optical Thickness
APF	Aerosol Phase Function
BOA	Bottom Of Atmosphere
IOP	Inherent Optical Properties
IOPA	Inherent Optical Properties of Aerosols
LUT	Look Up Table
MERIS	MEdium Resolution Imaging Spectrometer
NIR	Near-Infrared
PPL	Principal PLane
RMS	Root Mean Square error
SAM	Standard Aerosol Model
TOA	Top Of Atmosphere

Symbols

α	Angstrom coefficient
Θ	Scattering angle
τ	Optical thickness
ϖ_0	Single scattering albedo
$P(\Theta)$	Phase function
λ	Wavelength

m	Real part of the refractive index

1) INTRODUCTION

One key objective of ISECA is to promote the use of the satellite observation as a monitoring tool for water quality assessment. For a space borne sensor, the contribution of the atmosphere dominates the contribution of the ocean (blue). The clear atmosphere presents a large spatial homogeneity compared to the ocean. Therefore, the structures we see on the satellite imagery correspond to oceanic features at least in the absence of clouds.

The accuracy of this atmospheric correction is related to the knowledge of the aerosol optical properties. The objective of this report is to characterize the inherent optical properties (inherent = for an elementary scattering volume) of the aerosols in the *2Seas* region in order to have the suitable inputs to train the algorithms and/or to generate the required LUTs of the apparent optical properties (apparent = for the whole atmospheric layer).

The experimental tool is AERONET, section 2.

The theoretical tool is WOPAER, a software package developed at ADRINORD, to derive the aerosol phase functions from the sky radiance measurements provided by AERONET. We revisit here all the WOPAER processing chain in *section 2*.

2) THE AEROSOL APPARENT OPTICAL PROPERTIES FROM AERONET

2.1) The AERONET network

AERONET is a globally distributed network of automated ground-based instruments and data archive system, developed to support the aerosol community. The instruments used are CIMEL spectral radiometers that measure the spectral extinction of the direct Sun radiance (Holben *et al.*, 1998). The aerosol optical depths are determined using the *Beer-Bouguer* Law in several spectral bands.

The Figure 1 describes the apparent optical properties we measure with a ground-based radiometer. This radiometer is the CIMEL instrument which collects both extinction measurements (a) and sky radiances both in the principal plane (b; solar plane) and the almucantar (c).

From the Cimel measurements, we have seen previously (uper right corner of Figure 1) how to get the inherent optical properties which are the extinction coefficient and the phase fonction. Then, thanks to the IOPs, we can simulate (lower right corner of Figure 1) the CIMEL measurement and (the lower left corner of Figure 1) the satelitte signal or perform the atmospheric correction. Finaly (from lower left to upper left of Figure 1), we can validate the aerosol model used for the atmospheric correction in a comparison between CIMEL measurements and what this aerosol model predict.

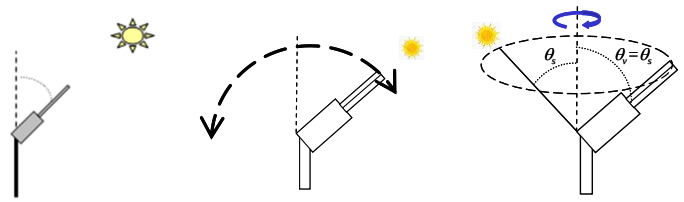

(a) (b) (c)

Figure 1: *Description of the different acquisition protocols of the CIMEL instrument.*

2.2) The AERONET data base

2.2.1 - *The 2Seas database*

In the A2 preparation phase, we identified and described the AERONET network in our area. A detailed description of the selected AERONET sites is available in (R1).

North Sea
Helgoland (54N,7E) - Start Date: 01-01-1999; Latest Date: 31-12-2007

Table 1:

The Hague (52N,4E) - Start Date: 01-01-2001; Latest Date: 31-12-2006
Oostende (51N,2E) - Start Date: 01-01-2001; Latest Date: 31-12-2007
Dunkerque (51N,2E) - Start Date: 01-01-2003; Latest Date: 31-12-2007
English Channel
Lannion (48N,3W) - Start Date: 01-01-2004; Latest Date: 31-12-2007
Rame Head (50N,47W) - Start Date: 01-01-1997; Latest Date: 31-12-1999

Distribution of AERONET sites in the 2Seas region with the name, the location and the period of acquisition.

We analyze now in depth the CIMEL measurements and more extensively the AERONET products.

In §2.2.2, we will use the extinction measurements, actually the AOT derived from them, for a first analysis. The AOT in one spectral band will inform on the aerosol abundance in the atmospheric column. A standard to evaluate is the horizontal visibility V. A visibility of 23 km is associated to an AOT at 675 nm of 0.15. The spectral dependence of the AOT is described by the Angstrom coefficient.

In §2.2.3, we will use the sky radiance measurements. The atmospheric correction algorithm requires auxiliary data. The LUTs of the atmospheric radiance, computed for standard aerosol models, is the key element. The retrieval of the CIMEL sky radiances by these aerosol models is a clear indicator of their ability to correctly describe the aerosol scattering properties.

The extinction and sky radiance measurements are used by the AERONET team to produce aerosol models. With these aerosol models, the aerosol inherent properties are computed as an AERONET product. In §2.2.4, we will use the AERONET phase functions to evaluate their ability to reconstruct the sky radiance. It is an important issue for ISECA because VITO will use this AERONET product to build a regional climatology in the 2Seas region.

2.2.2 - *The aerosol climatology from the extinction measurements*

For this study, *level 2* data are used and consist of AOT at 440, 675 and 870 nm, retrieved at least every 15 min during daytime. *Level 2* data are cloud-free and quality assured retrieved from pre- and post-field calibrated measurements (Smirnov *et al.*, 2000). The estimated accuracy in the AERONET AOT is between ±0.01 and ±0.02 and depends on the wavelength, for an air-mass equal to 1 (Dubovik *et al.*, 2000). We displayed in Figure 2 the spectral distribution of the AOT and of the *Angstrom* coefficient for each selected AERONET sites.

In Figure 2, we clearly retrieve common features between the different sites both in terms of AOT values (related to the abundance) as well as on the Angstrom coefficient (related to the size). As a consequence, in our 2Seas area, the aerosols likely present the same inherent optical properties. The retrieval of these IOPs can be conducted on a unique database that combines all the Cimel data.
This retrieval will be conducted using the WOPAER processing chain as described below.

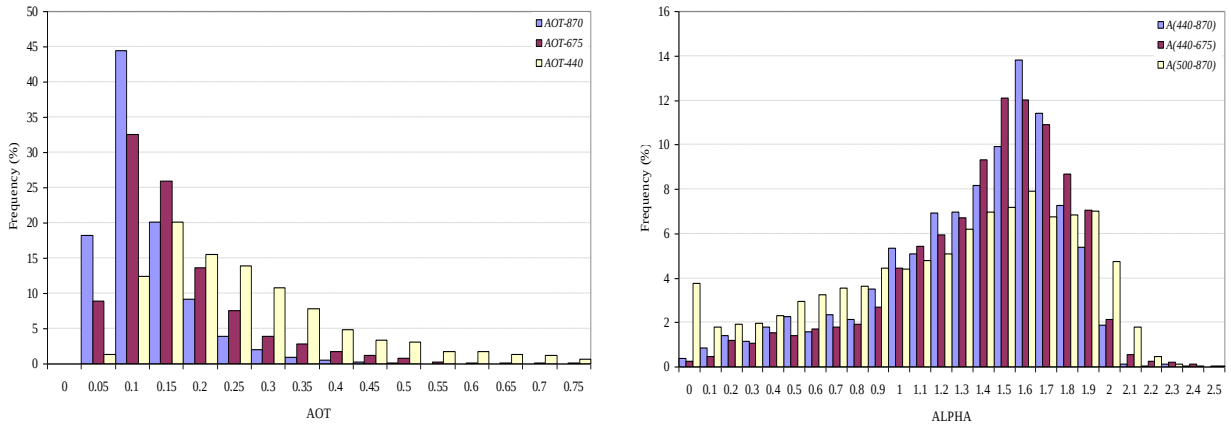

The Hague

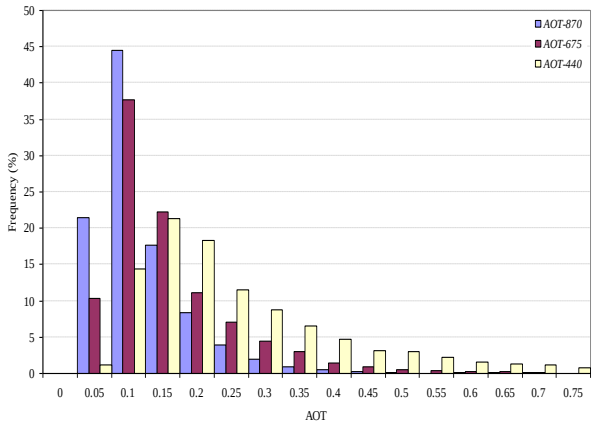

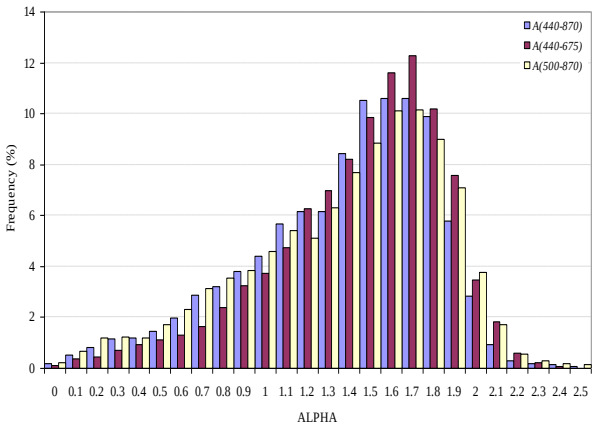

Oostende

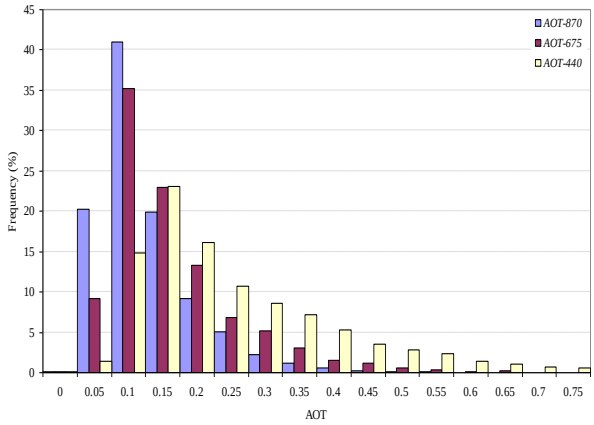

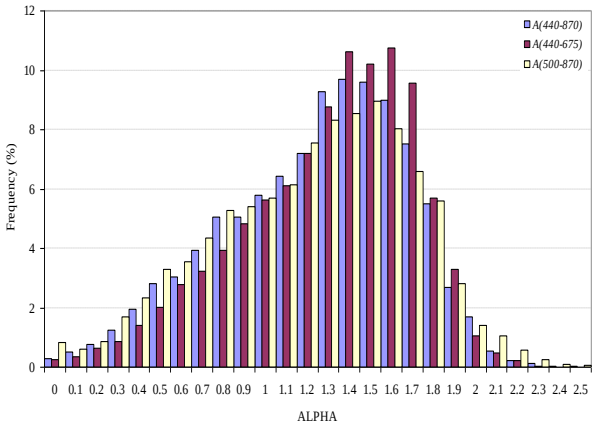

Dunkerque

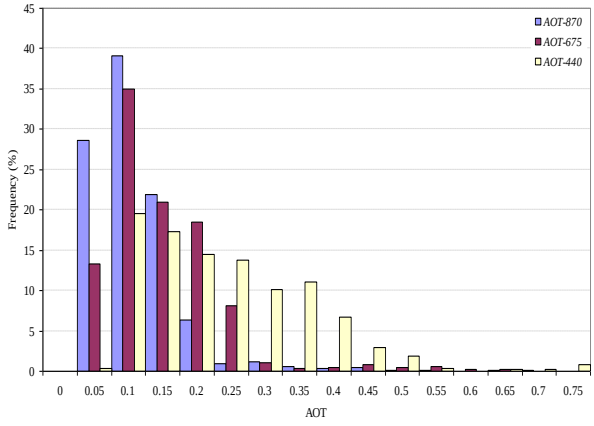

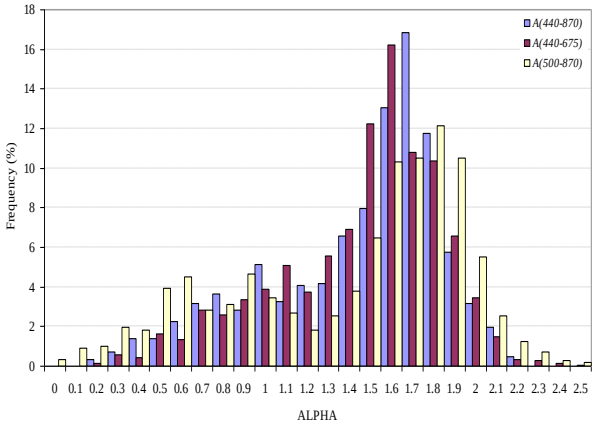

Lannion

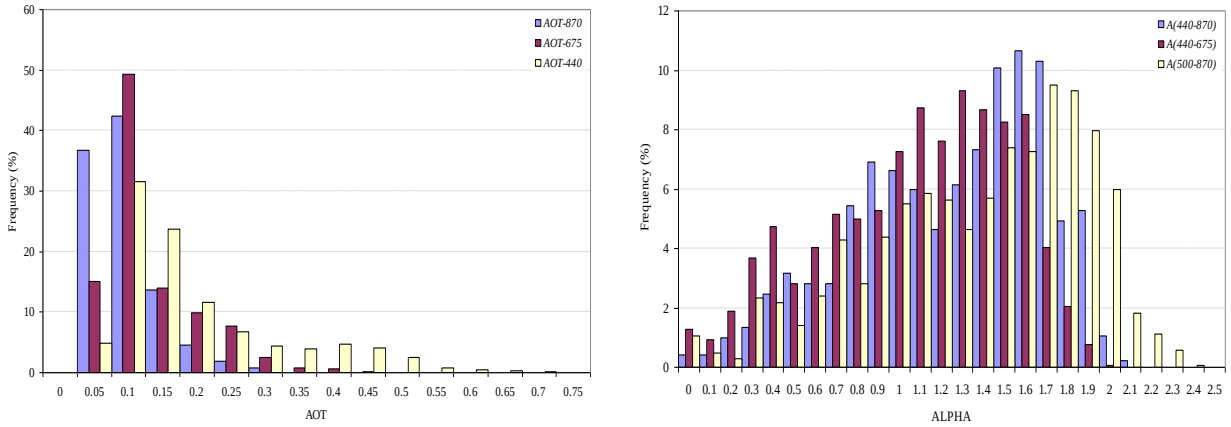

Rame Head

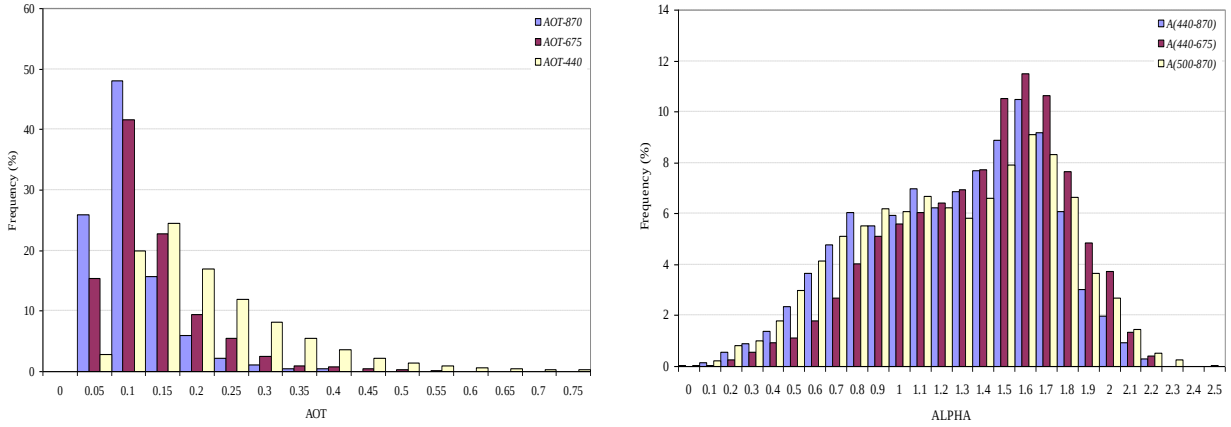

Helgoland

<u>Figure 2:</u> Histogram of the AOTs and Angstrom coefficients for the different AERONET sites.

The spatial homogeneity of the aerosols is also a second element. This task is conducted by associating the extinction measurements of two AERONET stations at the same time, within 10 minutes. Here, for Oostende and Lille, we have something like 10280 simultaneous measurements. The results are reported in Figure 2. We first plotted the AOT at 440 nm and 870 nm without data filtering. In mean, Lille appears more turbid than Oostende by a little more than 10 percent, which can be expected when comparing the size of their respective urban tissue.

If the AOT indicated the aerosol abundance, the Angstrom coefficient is linked to the aerosol size. The general similarity between Lille and Oostende values suggests a large spatial homogeneity of the nature of the aerosols.

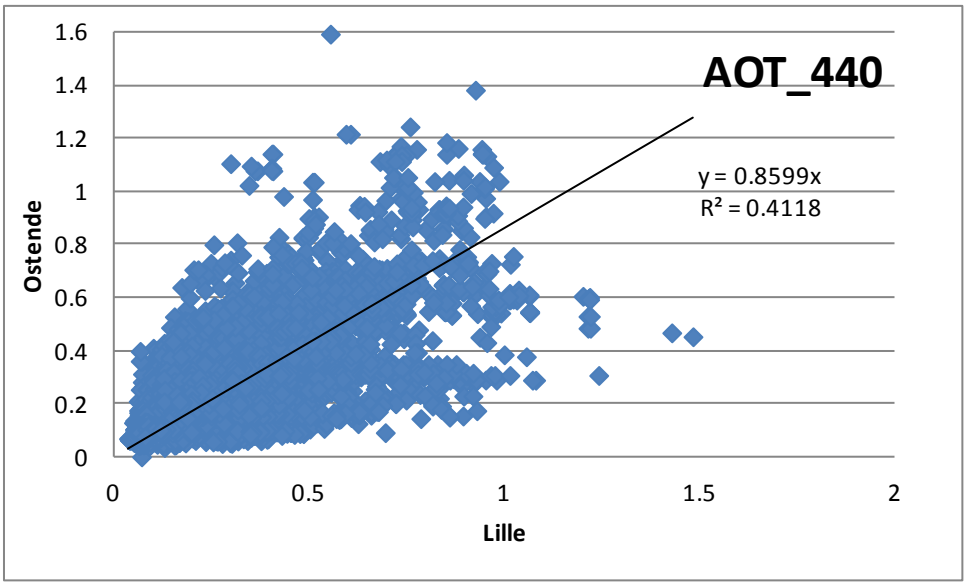

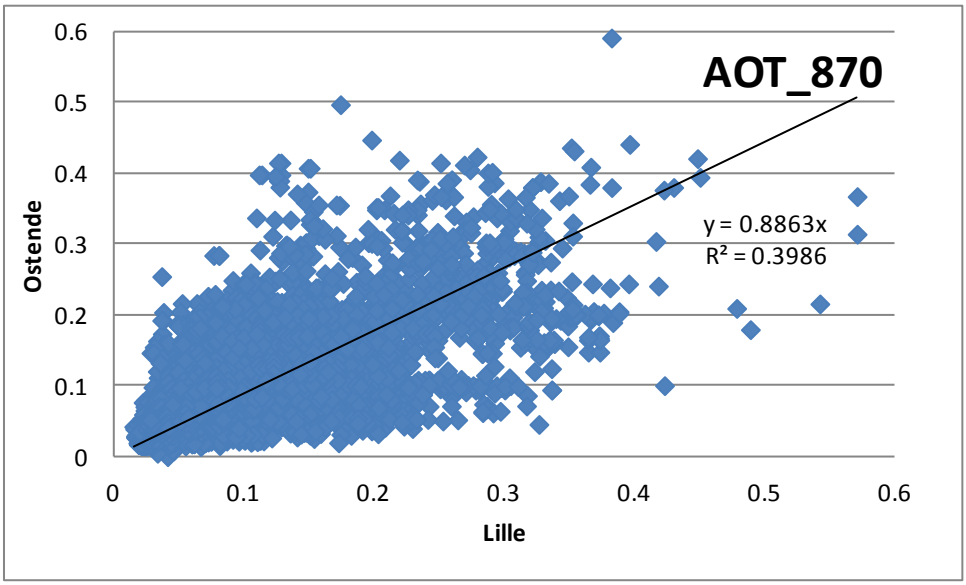

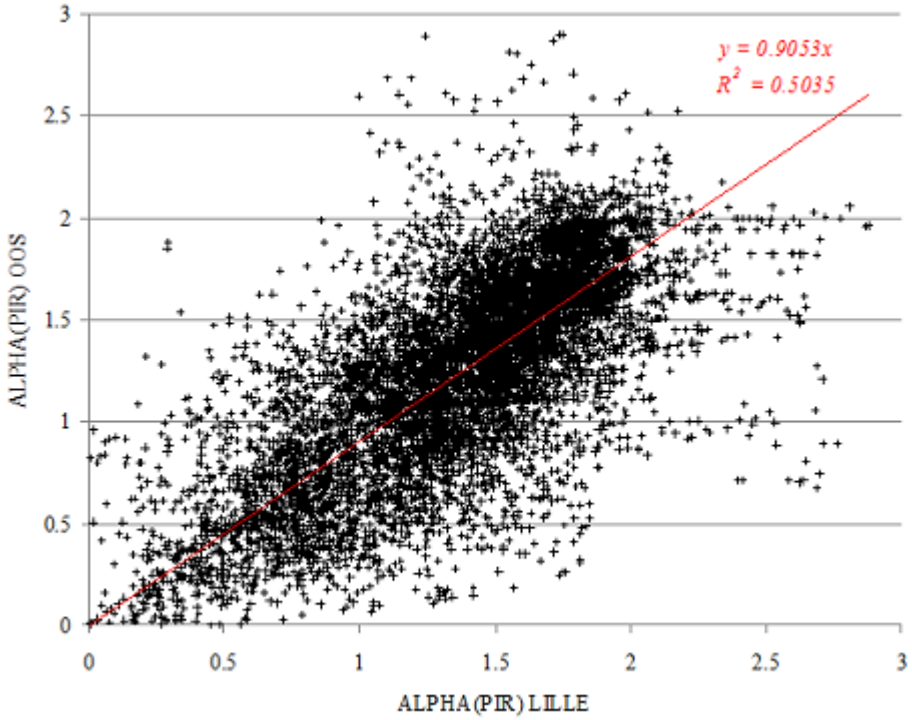

Figure 3: Correlation on the AOT between Lille and Oostende with from top to bottom: AOT at 440 nm, AOT at 870 nm and the Angstrom coefficient.

3 GENERATION OF THE INPUT FILE FOR WOPAER

3.1 – Downloading the CIMEL data

The first task is to download the Cimel data from the AERONET web site. In order to assure a quality of the data, lev2.0 (quality control data) are used. The native AERONET files are text file. The processing chain is in Fortran. It was necessary to identify the content and format to read the AERONET files. In order to give example of the content, we open the text file using excel. We downloaded from AERONET the Oostende data in May 2012. Table 2 applies to the extinction measurements with:

(a) The header

(b) The date-time information

(c) In the upper part, the AOT. N/A indicates here that there is no spectral band for this specific CIMEL instrument. The lower part corresponds to the dispersion in percent for 3 consecutive measurements.

(d) We have the precipitable water amount derived from the water vapour absorption at 940 nm.

(e) From the AOT, once can compute the dynamic Angstrom coefficient between two wavelengths.

Level	1.5.	Real	Time	Cloud	Screened
Version	2	Direct	Sun	Algorithm	
Location=Oostende	long=2.925	lat=51.225	elev=23	Nmeas=1	PI=Kevin_Ruddick

(a)

Date			Time			
d	m	y	hh	mm	ss	Julian_Day
7	5	2012	14	15	49	128.594317
11	5	2012	17	21	15	132.72309
11	5	2012	17	24	44	132.725509
12	5	2012	6	20	36	133.264306
12	5	2012	8	7	31	133.338553
12	5	2012	8	30	42	133.354653

(b)

AOT															
1640	1020	870	675	667	555	551	532	531	500	490	443	440	412	380	340
N/A	0.076642	0.106173	0.172392	N/A	N/A	N/A	N/A	N/A	0.263937	N/A	N/A	0.317554	N/A	0.3549	0.4072
N/A	0.058952	0.073864	0.107606	N/A	N/A	N/A	N/A	N/A	0.174961	N/A	N/A	0.219725	N/A	0.2649	0.30931
N/A	0.050202	0.062253	0.089639	N/A	N/A	N/A	N/A	N/A	0.145813	N/A	N/A	0.185636	N/A	0.2248	0.26576
N/A	0.024177	0.030937	0.045036	N/A	N/A	N/A	N/A	N/A	0.069456	N/A	N/A	0.091429	N/A	0.1063	0.13514
N/A	0.032841	0.042877	0.067313	N/A	N/A	N/A	N/A	N/A	0.102691	N/A	N/A	0.134221	N/A	0.1544	0.19878
N/A	0.030639	0.040208	0.065287	N/A	N/A	N/A	N/A	N/A	0.100227	N/A	N/A	0.132713	N/A	0.1513	0.19523
1640	1020	870	675	667	555	551	532	531	500	490	443	440	412	380	340
N/A	0.725896	0.634046	0.545068	N/A	N/A	N/A	N/A	N/A	0.10089	N/A	N/A	0.90133	N/A	0.5781	0.48558
N/A	0.145044	0.265556	0.454516	N/A	N/A	N/A	N/A	N/A	0.728783	N/A	N/A	0.796399	N/A	0.8231	0.89205
N/A	0.215805	0.350244	0.536126	N/A	N/A	N/A	N/A	N/A	0.889713	N/A	N/A	1.149755	N/A	1.2464	1.51223
N/A	0.110519	0.153993	0.257905	N/A	N/A	N/A	N/A	N/A	0.349457	N/A	N/A	0.450016	N/A	0.7398	0.83569
N/A	0.055827	0.083314	0.060806	N/A	N/A	N/A	N/A	N/A	0.079599	N/A	N/A	0.259699	N/A	0.315	0.15847
N/A	0.515567	0.35382	0.54131	N/A	N/A	N/A	N/A	N/A	0.642816	N/A	N/A	0.738332	N/A	0.8408	0.84532

(c)

Water(cm)
1.733253
1.511608
1.488186
1.073176
1.092181
1.15355

(d)

440-870Angs	380-500Angs	440-675Angs	500-870Angs	340-440Angs	440-675Angs	Last_Process	SZA
1.593878	1.057638	1.433701	1.644625	0.94466	N/A	9/5/2012	45.413526
1.602293	1.487224	1.668572	1.565311	1.31223	N/A	13/05/2012	72.309394
1.602645	1.552266	1.696098	1.545599	1.375065	N/A	13/05/2012	72.848062
1.560791	1.519778	1.626075	1.465851	1.475355	N/A	14/05/2012	70.259128
1.63432	1.453961	1.584907	1.578671	1.478388	N/A	14/05/2012	53.71203

(e)

Table 2: the AERONET AOT file

Separately, we downloaded the radiance measurements in the principal plane. Table 3 tells us that the measurements are acquired in 4 spectral bands. Some are excluded after a quality control test. When we have the 4 bands, the 4 bands are acquired in less than 2 minutes. Figure 4 reports the sky radiance. It seems that the measurements at 1020 nm are quite noisy certainly because we are at the spectral edge of the detector for small signal.

Date			Time				
d	m	y	h	mm	s	Wavelength	SZA
1	5	2012	10	54	53	1.0201	37.342323
1	5	2012	11	47	4	1.0201	35.933415
1	5	2012	11	47	45	0.8701	35.934853
1	5	2012	17	4	9	1.0201	71.636074
1	5	2012	17	4	51	0.8701	71.745216
6	5	2012	14	46	39	1.0201	49.774365
6	5	2012	14	47	26	0.8701	49.883836
6	5	2012	14	48	16	0.675	50.000502
6	5	2012	14	49	8	0.4409	50.12206

Table 3: Characteristic of the principal plane sequences

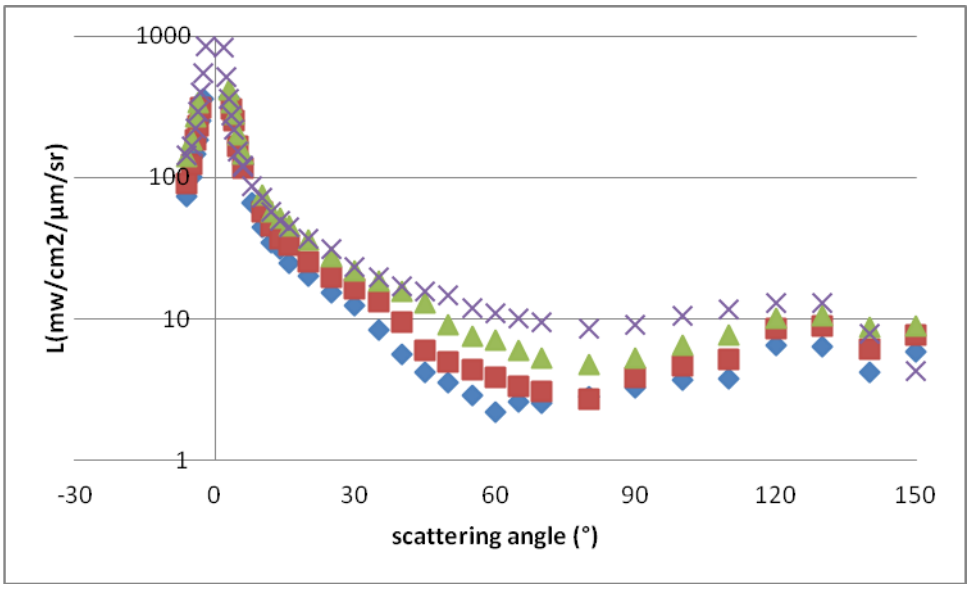

Figure 4: Measurements on May 6, 2012 around 14h50 in Oostende of the sky radiance in the principal plane in four spectral bands (1020=blue diamond; 870=red square; 675=green triangle; 440=violet cross)

Finally, we downloaded the radiance measurements in the almulcantar. Table 4 tells us that the measurements are acquired in 4 spectral bands in less than 2 minutes but that they are simultaneous to the principal plane measurements. Figure 5 reports the sky radiance. It seems that the measurements at 1020 nm are quite noisy certainly because we are at the spectral edge of the detector for small signal.

Date			Time				
d	m	y	h	mm	s	Wavelength(µm)	SZA
6	5	2012	12	47	4	1.0201	36.637178
6	5	2012	12	48	32	0.8701	36.73662
6	5	2012	12	50	5	0.675	36.843912
6	5	2012	12	51	35	0.4409	36.949876
6	5	2012	15	16	36	1.0201	54.080139
6	5	2012	15	18	16	0.8701	54.326091
6	5	2012	15	20	3	0.675	54.589891
6	5	2012	15	21	43	0.4409	54.83701

Table 4: Characteristic of the almulcantar sequences on May 6, 2012

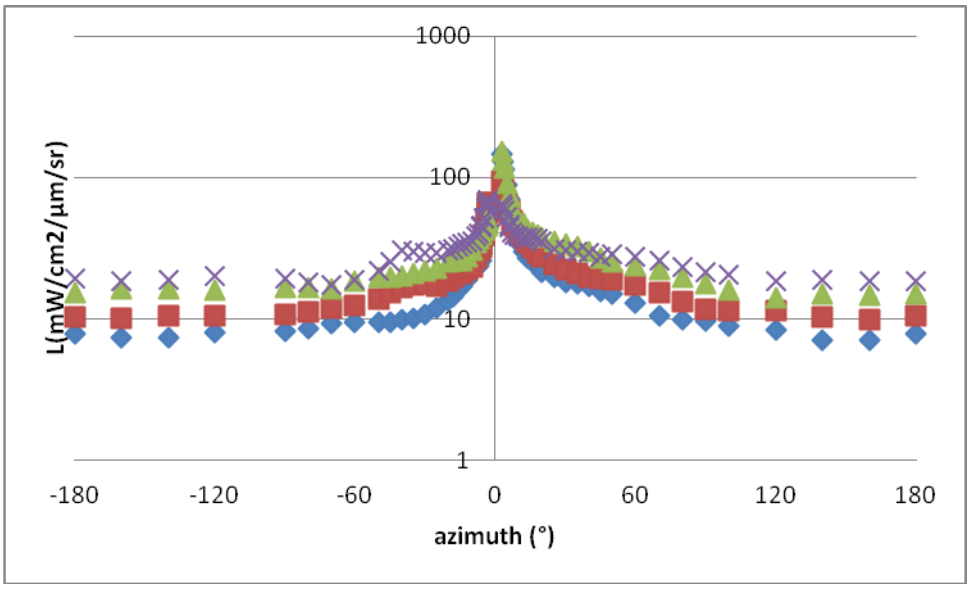

Figure 5: same as Figure 4 but for the almulcantar on May 6, 2012 around 12h50

Note that it should be interesting

(i) To add the water vapour content information (see table 2d) first for analysis of the aerosol IOP (the aerosol size is sensitive to the humidity) and second as a potential input for a more accurate gaseous correction.

(ii) To use the OATs to derive the spectral dependence of the extinction coefficient. For MERIS, we need to have this spectral dependence in 15 spectral bands with a normalisation at 550 nm. A simple module using a spline line should easily provide this information. Figure 6 gives the AOT for the three days of table 2. With such a good spectral continuity, we can predict the AOT in all the MERIS band directly or in a log-log scale.

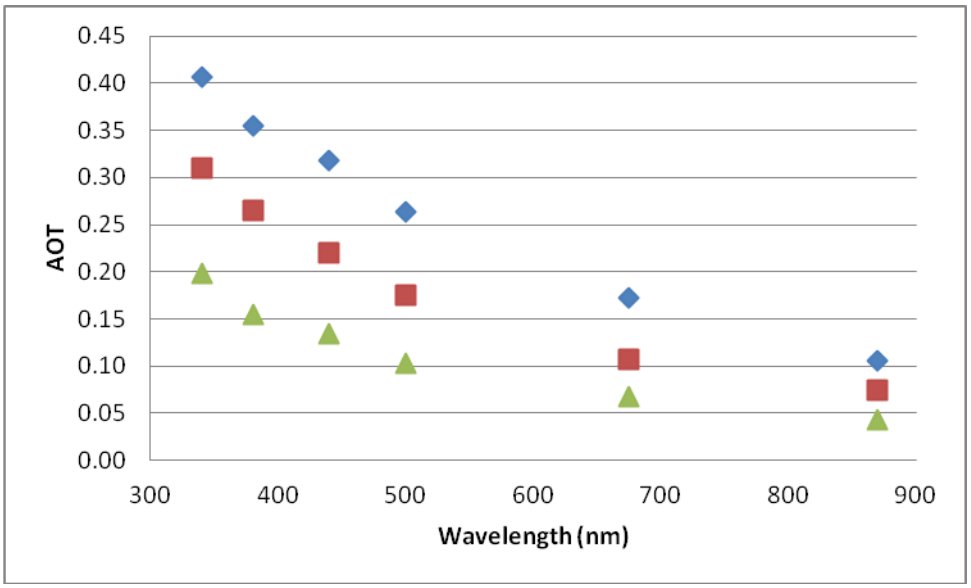

Figure 6: Spectral dependence of the CIMEL AOT

3.2 – Selection of the sky radiance measurements in the almulcantar

For the almulcantar, if the atmosphere is homogeneous, we should have a symmetry from the principal plane. To ensure a spatial homogeneity of the measurements during the almucantar acquisition, we set a symmetry threshold (ratio between two sequences; Figure 6) of 20 %.

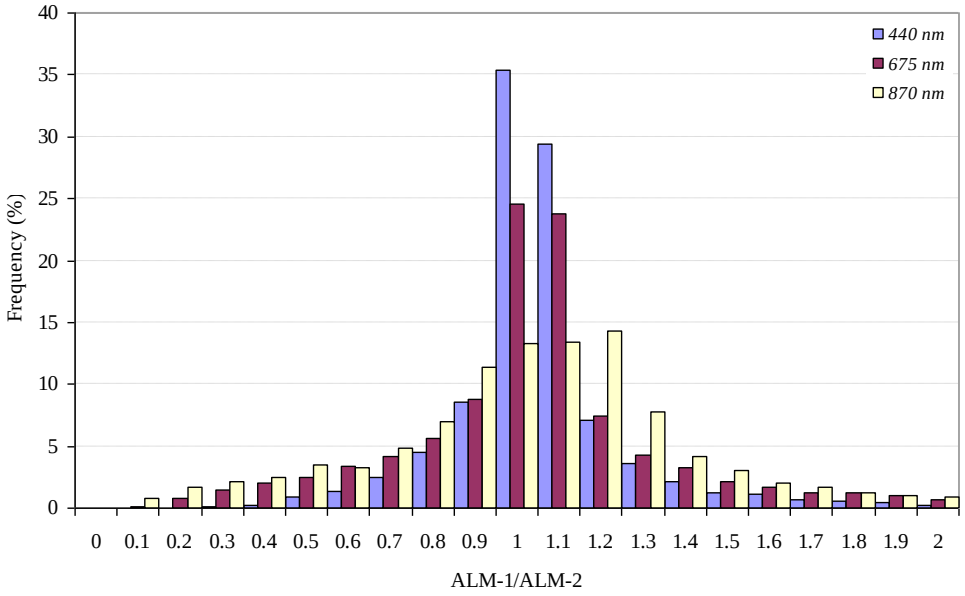

Figure 7: Histogram of the relative difference between the two almucantar scans (phi = 120°) in the three spectral bands for the Oostende AERONET site.

Applying this threshold on the *Oostende* AERONET site (representative of our ocean set), we have (Figure 7):

- At 440 nm: 90 % of the sequences.
- At 675 nm: 80 % of the sequences.
- At 870 nm: 65 % of the sequences.

As an illustration, we summarized in Table 6 the number of sequences after each filtering step:

- Step 1: Initial data set.
- Step 2: After applying the four types of criteria.
- Step 3: After applying the new wopaer quality control test.

		440 nm	675 nm	870 nm
PPL	Step 1	8210	6617	7020
	Step 2	5926		
	Step 3			
ALM	Step 1	9331	11021	10567
	Step 2	8214		
	Step 3			

Table 6: Number of sky radiance sequences selected for each site over ocean in the principal plane and in the almucantar for each wavelength: initial data set (step 1), after a first filtering (step 2) and after wopaer filtering (step 3).

3.3 The WOPAER input file

WOPAER will be described in details in section 4. The inputs to WOPAER combined the CIMEL AOTs and radiance measurements.

The interpretation of the Cimel radiance is done using the SOS code which outputs normalized radiance (solar irradiance equal to π) without gaseous absorption. The first task is then to correct the Cimel radiance measurements from the gaseous absorption and to normalize them.

Correct from the gaseous absorption

The gaseous absorption can be neglected in the CIMEL spectral bands except for the ozone and this mainly at 675 nm. The ozone absorption is corrected with:

$$L_{ng}^{*} = \frac{L^{*}}{T_{o3}} \quad (1)$$

The ozone transmittance T_{O3} is given by:

$$T_{o3} = \exp\left(- \frac{U_{o3}\,\tau_{o3}}{0.35\cos(\theta_s)} \right) \quad (2)$$

The amount of ozone U_{O3} corresponds to OMI (sensor) monthly climatologic values provided by latitude by steps of 10°. The solar zenith angle θs is in the data file. Table 6 gives the ozone optical thicknesses τ_{O3} computed for a standard value of 0.35 cm.atm.

λ (nm)	440	670	870
E_s (w/m²/µm/sr)	1928.267	1566.065	987.366
τ_{O3} (for 0.35cm.atm)	0.00400	0.04685	0.00485

Table 6: *Solar irradiance and ozone optical thickness in the 3 CIMEL bands.*

NB: In AERONET inversion products (V2.0), the amount of ozone is provided using NASA Total Ozone Mapping Spectrometer (TOMS; Earth Probe and Nimbus) with a spatial resolution of 1 x 1.25 degrees. An update of the processor should use the same information

Convert the sky radiance into a normalised radiance

We did not use the spectral band at 1020 nm for the following reasons:

(i) For MERIS, using 870 nm is sufficient.

(ii) The sky radiance at 1020 nm can be low in the backscattering and the poor performance of the detector induces noise.

(iii) There is a temperature effect even if a correction is applied.

The sky radiance L (w/m²/µm/sr) is converted into normalized radiance with:

$$L^{*} = \frac{\pi\, L_{1B}}{E_S^J} \quad (3)$$

Where the denominator is the solar irradiances corrected form the Earth-Sun distance (in UA) at the Julian day *J* and given by:

$$E_S^J = \frac{E_S}{\left[A - B\cos\left(\frac{2\pi(CJ - D)}{E} \right) - 0.00014\cos\left(\frac{4\pi(CJ - D)}{E} \right) \right]^2} \quad (4)$$

Where: A=1.00014; B=0.01671; C=0.9856002831; D=3.4532868; E=360; the solar irradiances *Es* are reported in Table 6.

Insert the AOT in the sky radiance

Starting with the AERONET files, a site is first selected and for a given band (chosen among 440, 675 and 870 nm) the AOT is interpolated at the time of the sky radiance sequence and the dynamic Angstrom coefficient (actually -α) is provided between 670-870 nm and between 440-670 nm. No check on the proximity between the times of acquisition

of radiances and irradiances are performed. It is recommended to check if the two irradiance sequences which bound the sky radiance measurements are within less than half an hour.

3.4 – General flow chart

We download from AERONET 3 files. Here for Oostende and May 2012, we have explicit file name:

(i) AOT: 120501_120531_Oostende.lev15

(ii) 120501_120531_Oostende.ppl

(iii) 120501_120531_Oostende.alm

Let us follow for the PPL the flowchart of figure 8:

(i) We open the "120501_120531_Oostende.ppl" file.

(ii) We read the current line (starting by the first) of this file It corresponds to one sequence of sky radiance measurements in one spectral band.

(iii) We open the AOT in "120501_120531_Oostende.lev15" file.

(iv) We read in a loop the AOT in "120501_120531_Oostende.lev15" to find the time coincidence with the ppl line.

(v) If we have this matchup AOT-L, we resume processing L with the O3 correction and the normalisation.

(vi) At the end, we merge AOT and L

(vii) We close the AOT file before going to the next line in the L file.

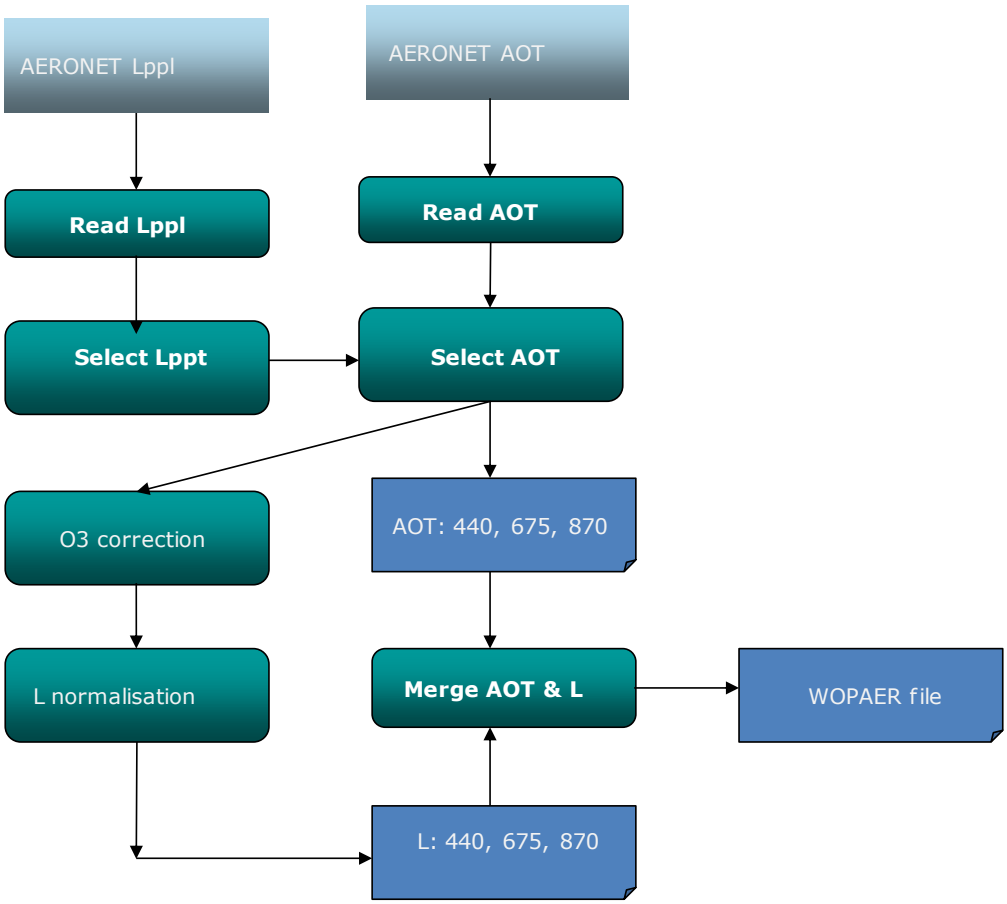

Figure 8: Generation of the PPL input file for WOPAER

The flow chart is a little different for the almulcantar, figure 9. First,a second test is made on the symmetry after the test of the coincidence between AOT and L. Second, we generate at the end two WOPAER files

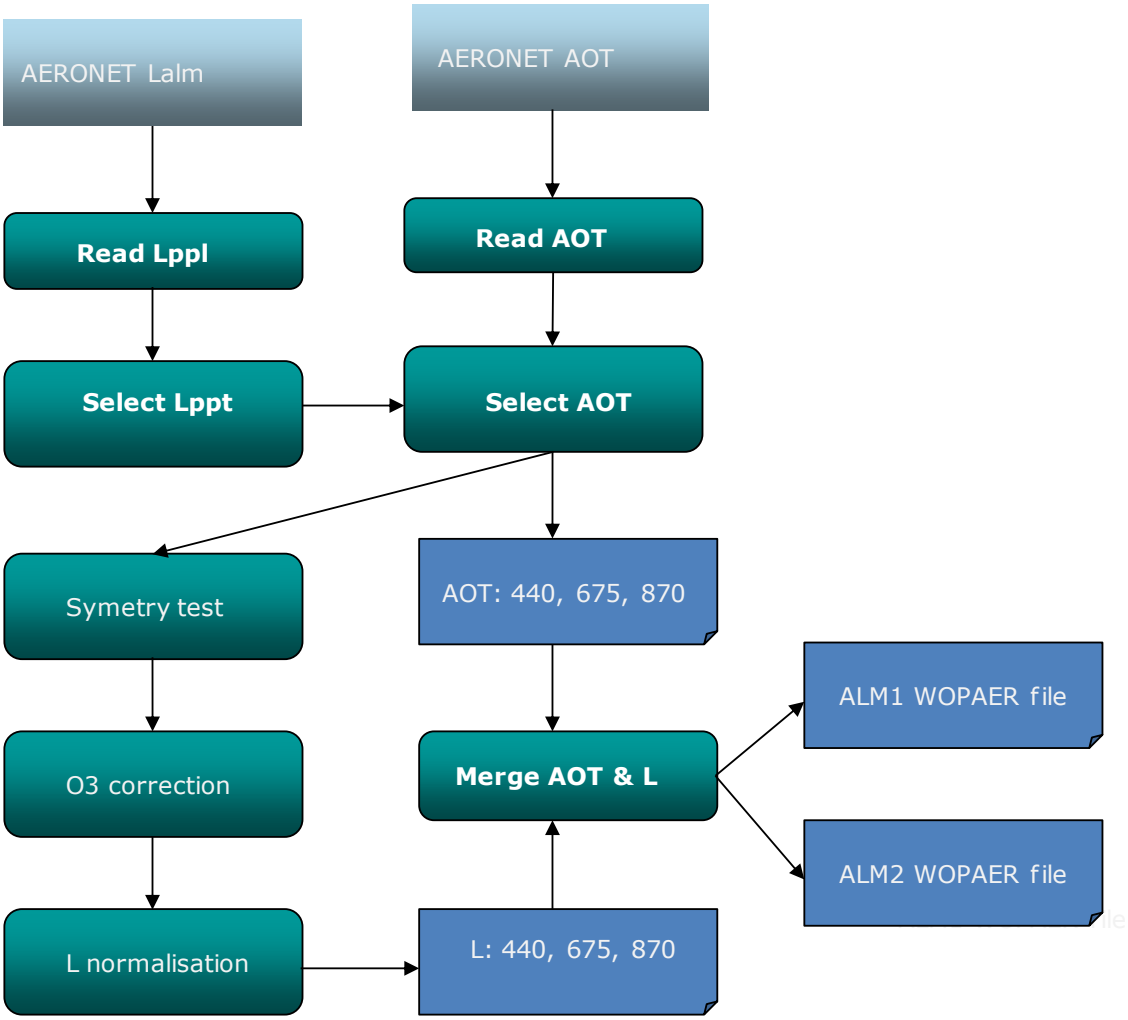

all the sky radiances for one site and for one band are stored in the same file. One line corresponds to one sequence.

4 WOPAER PROCESS

4.1) Selection of the sky radiance measurements

Three types of criteria are applied:

- *On the measurements*: In order to study the spectral dependency of the phase function, we want to have a set of sky radiance measurements in the 3 bands quite simultaneously. The test implemented rejects series of sky radiances with an interval between measurements at 440 nm and 870 nm (and 670 nm) larger than 0.1 hour. In order to have the full set of scattering angles between 2° and 150°, we process sequences at low solar elevations with:

$$65° \le \theta_s \le 75° \quad (5)$$

- *On the type of aerosols*: The classification of the aerosol IOPs will be based on the Angstrom coefficient (α). Over the ocean, the aerosol model is selected between the red and the NIR. Therefore, we use α(670,870). We bounded α in the interval:

$$-2.5 \le \alpha \le 0.5 \quad (6)$$

- *On the limitation of the phase function retrieval*: We do not expect to accurately retrieve the aerosol phase function if the AOT is too small. The limit in the 3 bands is:

$$\tau_a \ge 0.02 \quad (7)$$

On the other extreme, the retrieval scheme does not work when combining to large solar angles and too large AOT. The following criteria are used:

$$\text{At 440 nm: } \frac{\tau_a}{\mu_s} \leq 1.5 \quad (8)$$

$$\text{At 670 nm (or 870 nm): } \frac{\tau_a}{\mu_s} \leq 2.5 \quad (9)$$

4.2) WOPAER in brief

The SOS code (R-3) is our RTC. In the version we use, the vertical distributions of the molecules and of the aerosols follow an exponential law driven by the vertical scale height (8 km for the molecules, 3 km typically for the aerosols). Inputs are the wavelength, the *Rayleigh* and aerosol optical thicknesses, the aerosol phase matrix and the single scattering albedo. The land surface and the water body are *lambertian*. The *Fresnel* reflection over water is driven by the *Cox and Muck* model for the wave slope distribution.

The SOS code outputs are the sky radiances in any azimuth and at the 24 *Gaussian* angles used for the RTC angular integration in zenith. These outputs can rescaled at the CIMEL angles or at the 80 *Gaussian* angles required by WOPAER to expand in a *Legendre* series the aerosol phase functions. Another output from the SOS code is the diffuse irradiance.

The SOS code is a subroutine to WOPAER. At the WOPAER first order, the SOS code runs with the CIMEL AOTs and a standard aerosol models chosen in an aerosol family. A standard family for land measurements is associated to the Angstrom coefficient through a *Junge* power law. A standard aerosol refractive index for continental material is 1.44 with an imaginary part of 0.005. The *Mie* theory is used to compute the scattering phase matrix. With this aerosol type, the measured AOT, the barometric pressure for the *Rayleigh* computation, an assumed surface albedo, we compute the ratio *f* between the primary scattering and the sky radiance.

This ratio is applied to the sky radiance measurement to first get the primary scattering and second the aerosol phase function. The maximum scattering angle Θ collects by the CIMEL is 150°. The maximum reaches in the principal plane is $90° + \theta_s$. We want to avoid grazing view angles larger than 75° in order to still be in the plane parallel approximation, then $\Theta < 75° + \theta_s$. To expend the aerosol phase function into a *Legendre* series, we need to extrapolate Θ up to 180°. It is done with the 0^{th} phase function (first guess).

The following iteration computes the ratio *f* to get a new aerosol phase function. The convergence is made on the relative variation on *f* between the two successive orders of iteration. We retain the maximum value and stop the iteration when $(\Delta f/f)_{max} < 1$ percent. If this criterion is not reach after 30 iterations, we stop iterating.

At convergence, WOPAER returns the single scattering albedo, the aerosol phase function and the diffuse irradiance as basis products. As break points, we output also:

(*i*) The maximum, minimum and mean value of the relative difference between the measured sky radiance and it prediction at order zero.

(*ii*) The same values but at the order of convergence.

4.3 WOPAER improvements

4.3.1) The forward scattering issue

The CIMEL nominal field of view is +/-1 deg; (http://www.cimel.fr/photo/pdf/ce318_fr.pdf). The first scattering angle to collect the sky radiance in the principal plane is 2 deg. Therefore we should not have direct solar beam entering in the collimator with a Sun having an apparent diameter of 52 minutes. Nevertheless, when combining the uncertainty on the CIMEL FOV to error on the pointing, it may happen that for the first scattering angle of 2 deg. We have a contamination by the direct solar beam.

In the principal plane, a suspicion forward peak is often recorded (Figure 5) with almost a factor 10 between 2.5 deg; and 2 deg. This forward scattering issue has a direct impact on our retrieval chain (Figure 6).

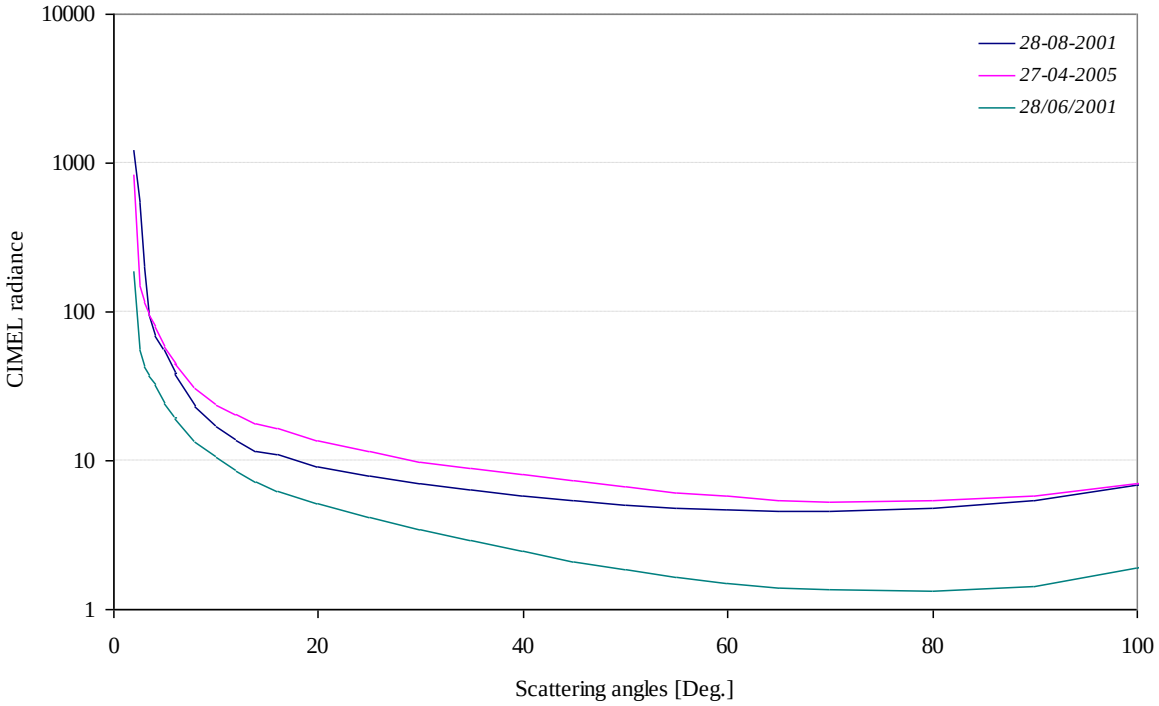

Figure 5: *Examples of sky radiance in the forward scattering as measured by CIMEL in the principal plane.*

Sky radiance and phase function are proportional in the forward peak. Figure 6 reports the phase function for 4 aerosol models. These models correspond to a power law for the size distribution and to a refractive index of 1.44. The slope of the power law is related to α.The phase function increases when α decreases but not as sharp as measured some time. In the near forward scattering, in this logarithmic plot the slope is near to one as confirmed by table 4. We computed the slope between 1.7 and 3.9 deg; and 3.9 and 6.2 deg to report the ratio in table 4.

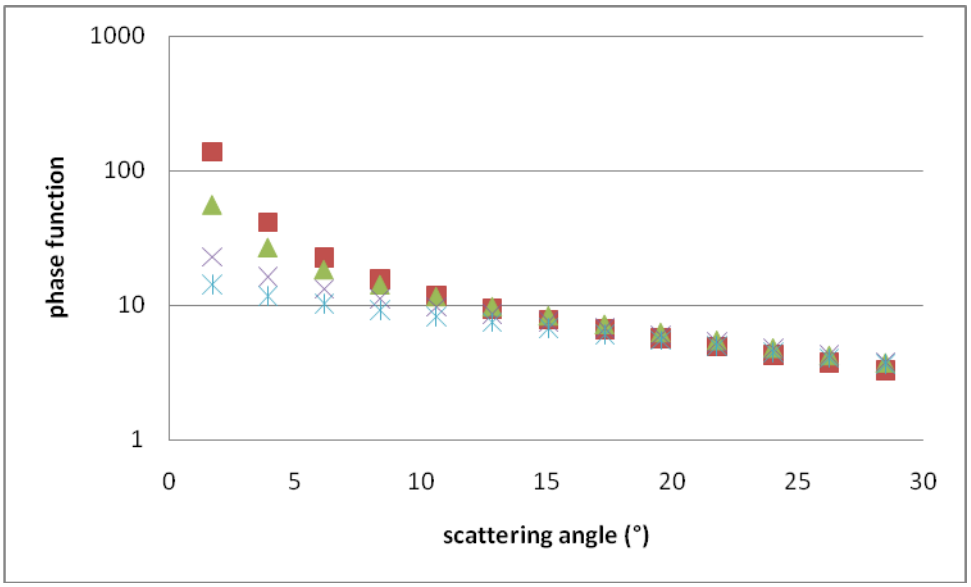

Figure 6: *Examples of phase functions with α=-2 (double cross),-1.5.(cross), -1 (green triangle) and -0.4 (red square)* .

α	-0.4	-1	-1.5	-2
ratio	1.09	1.05	0.91	0.77

Table 4: *For the 4 aerosol models, identified by α, we reported the ratio of the log slope of the aerosol phase function between two consecutive pairs of scattering angles (see text)*

The difference between two CIMEL consecutive measurements can be important in the forward scattering. There is a factor 10 between 2 and 2.5 deg of scattering angle in the sequences acquired on the 28-08-2001 and the 28-06-2001 (Figure 7). It does not correspond to what we expect.

In order to validate the credibility of the Cimel measurement at 2 deg., we have introduced a new criterion.

$$\frac{\log\left(\frac{L(2.0°)}{L(2.5°)}\right)}{\log\left(\frac{L(2.5°)}{L(3.0°)}\right)} \geq 2 \qquad (10)$$

If the Equation (10) is verified, we extrapolate the value of the radiance at 2.0° using the radiance values at 2.5° and 3.0 °

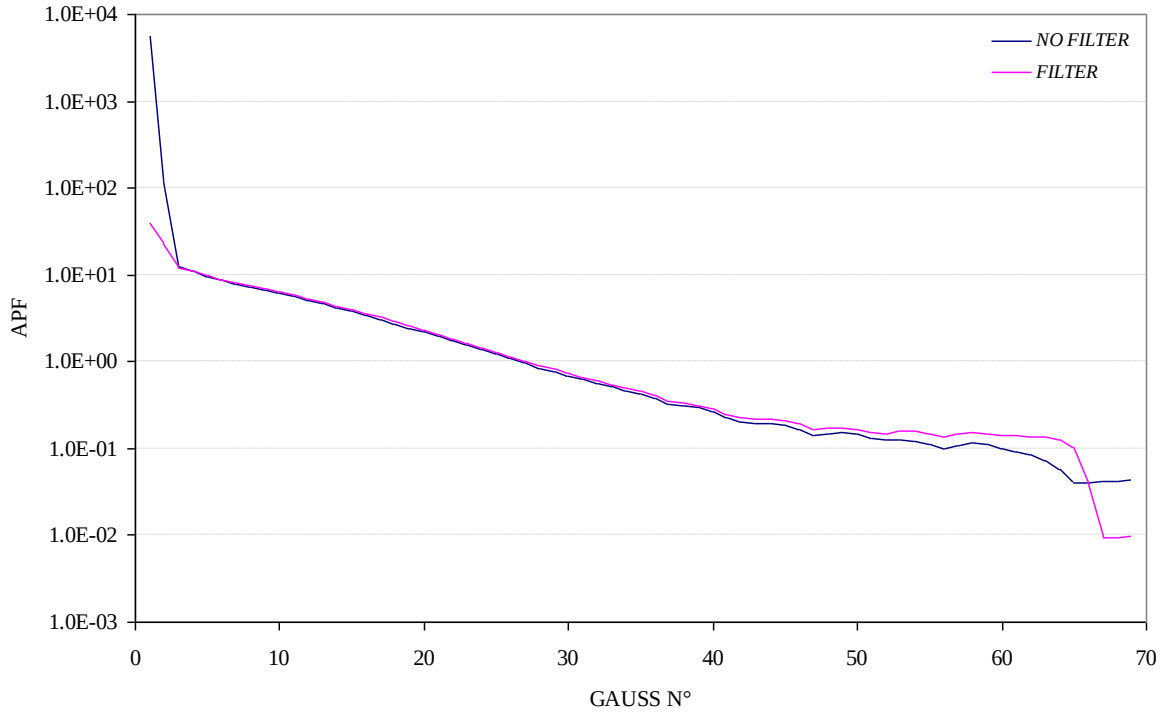

Figure 8*: The truncature: consequences on the retrieval of the phase function*

4.2.2) The solar angle issue

With the rough ocean as boundary condition, the standard version of the SOS code only works when the SZA corresponds to one of the 24 Gaussian angles used for the angular integration of the radiation field. In line with this angular integration the reflection matrix is computed for these 24 Gaussian angles. For WOPAER, at a given SZA, the SOS computation is done for the Gaussian angle just below. For example if the SZA is 75 deg., the SOS computation is done at 73.3 deg.

In WOPAER, the key computation is the ratio between multiple scattering and single scattering: *f*.

The relative error on *f* when computing with 73.3 °, instead of 75°, is reported in figure 8 for a principal plane computation. The aerosol model is associated to α=-1.5 associated to an AOT of 0.3 at 550 nm. A positive VZA corresponds to the forward scattering; the error on the SZA mostly impacts on the forward scattering because of the strong variability of the phase function.

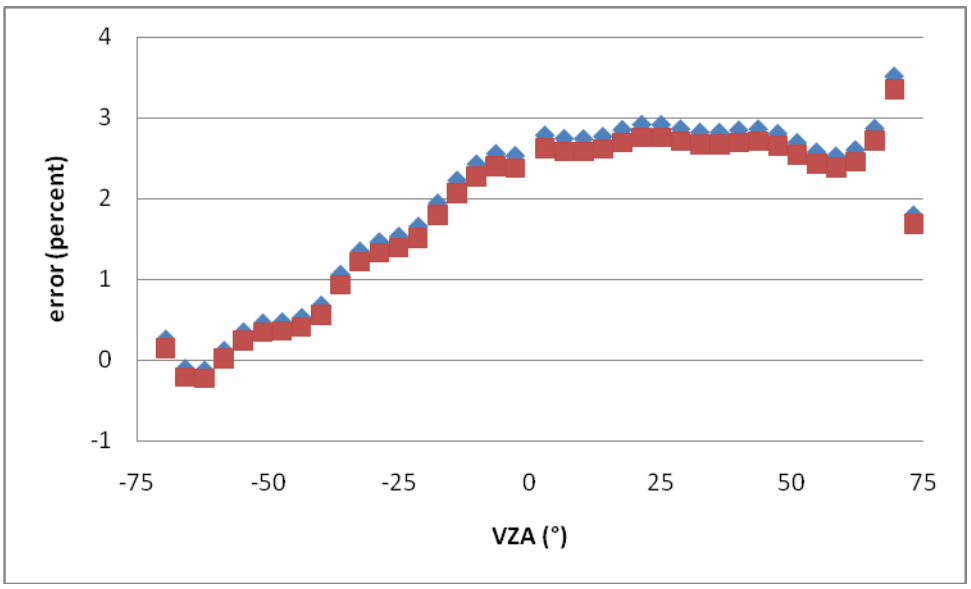

Figure 8: *Error on f as the relative difference between a computation at 75 deg compared to 73.3 deg..The influence of the wind speed is negligible with 3 m/s (blue triangles) and 7.2 m/s (red square)*

f allows converting the sky radiance into a phase function resulting of the mixing between the aerosols and the molecules. The mixing ratio w_0P depends on the solar angle and at a second order of the view angle. Therefore, when the SZA is actually 75 deg. and when we compute with the Gaussian angle at 73.3 deg., we commit an additional error as illustrated in Table 5.

73.3		75	
wPaer	wPray	wPaer	wPray
3.19E-02	2.60E-03	3.06E-02	2.55E-03

Table 5: *For At 865 nm, we reported the respective weights to the two phase functions, with the aerosol model used for Figure 11, at two SZAs.*

4) Conclusion and perspectives

We have a database in the 2Seas region of optical measurements dedicated to the characterization of the aerosols.

We did improve our processing chain devoted to the retrieval of the aerosol IOP in two steps:

(i) A better quality and improvements of WOPAER, the inversion tool.

(ii) An improved statistical tool to generate the IOP by class of aerosols. This tool needs to be made more operational.

We have a complementary database available through AERONET of the aerosol IOPs.

The next steps are:

(i) To generate the aerosol LUTs required to process MERIS images. This generation will be made with the global aerosol IOP (the global IOPA data base), the 2Seas regional IOPA database and the AERONET regional IOPA database.
(ii) To evaluate the performance of the MERIS atmospheric correction with the data sets. This evaluation will be made with in situ measurements.

5) References

Dubovik O., M. D. King, B. N. Holben, Y. J. Kaufman, A. Smirnov, T. F. Eck, and I. Slutsker A flexible inversion algorithm for retrieval of aerosol optical properties from Sun and sky radiance measurements, *J. Geophys. Res.*, 1999